RESEARCH ARTICLE

Synthesis and Evaluation of Radioiodine-Labeled pH (Low) Insertion Peptide Variant 7-Like Peptide as a Noninvasive Tumor Microenvironment Imaging Agent in a Mouse MDA-MB-231 Triple-Negative Breast Cancer Model

FengYu Wu[1], YueHua Chen[1], DaCheng Li[1], ZhenGuang Wang[1], and MingMing Yu[1]

[1]Department of Nuclear Medicine, The Affiliated Hospital of Qingdao University, No.59, Haier St., Laoshan District, Qingdao 266100, China 2022

Abstract

Purpose: The pH (low) insertion peptide (pHLIP) family can target the tumor microenvironment (TME). If pHLIP can be labeled with radioiodine, the imaging and treatment of tumors can be considered. However, tyrosine and tryptophan can bind with iodine in the insertion region of pHLIP, and radioiodine labeling may affect the formation of α-helix structures in acidic environments; therefore, it is necessary to adjust the structure of pHLIP. This study aims to develop an ^{125}I-labeled pH (low) insertion peptide variant 7-like peptide (pHLIP (Var7) LP) for imaging the TME in MDA-MB-231 triple-negative breast cancer (TNBC) xenograft tumor models.

Procedures: Based on pHLIP (Var7), a new peptide sequence, pHLIP (Var7) LP, was obtained by the sequence modification method and then characterized. The binding of pHLIP (Var7) LP to MDA-MB-231 cells was analyzed. pHLIP (Var7) LP was labeled with ^{125}I by the iodogen iodination method. Serial biodistribution studies and small-animal single photon emission computed tomography (SPECT)/ computed tomography (CT) imaging in subcutaneous MDA-MB-231 TNBC-bearing mice were performed using [^{125}I] I-pHLIP (Var7) LP.

Results: A novel peptide, pHLIP (Var7) LP, has the characteristics of an α-helix structure, electronegativity, and amphiphilicity. Circular dichroism (CD) spectroscopy showed that the peptide presented a typical pH-dependent transition from an unstructured conformation to an α-helix structure when the pH was reduced from 8.0 to 4.0. The relative fluorescence intensities of 5-carboxytetramethylrhodamine (5-TAMRA)-pHLIP(var7) LP at pH = 6.0, 6.6, and 7.4 were 100.00 ± 5.98%, 72.10 ± 4.65%, and 13.72 ± 1.41%, respectively. The distribution of [^{125}I] I-pHLIP (Var7) LP in tumors reached the highest level (8.7 ± 1.6% ID/g) at 2 h after injection, and the tumor-to-muscle ratios and tumor-to-blood ratios increased with time. Of the measured off-target organs, the stomach, kidney, and bladder showed higher uptake levels. SPECT imaging revealed rapid and sustained tumor uptake of [^{125}I] I-pHLIP (Var7) LP in breast cancer-bearing mice.

Conclusions: This study showed that [^{125}I]I-pHLIP (Var7)LP had rapid and sustained tumor uptake in MDA-MB-231 TNBC and provided a new method for TNBC imaging and further treatment.

Key words pH (low) insertion peptides · Sequence modification method · Triple negative breast cancer · Iodine-125 · Small-animal SPECT/CT

Correspondence to: MingMing Yu; *e-mail: mingmingyu@ bjmu.edu.cn*

Introduction

Triple-negative breast cancer (TNBC) is a subtype of breast cancer with molecular diversity. These tumor cells lack the expression of estrogen receptor (ER), progesterone receptor (PR), and human epidermal growth factor receptor 2 (HER-2) [1, 2]. TNBC accounts for approximately 12 to 17% of all breast cancers. In routine clinical practice, the imaging diagnosis of breast cancer mainly relies on mammography (MG), magnetic resonance imaging (MRI), and ultrasonography [3]. However, TNBC is more common in young women [4, 5]. The breast tissues of this population are relatively dense, and the sensitivities of MG and ultrasonography are thus low [6]; although the sensitivity of MRI is relatively high, the false positive rate is high [7]. Because of the lack of specific molecular targets, chemotherapy is currently the only option for the treatment of metastatic TNBC [8], but chemotherapy can have severe side effects including neutropenia, diarrhea, nausea/vomiting, myalgia, fatigue [9], the reactivation of hepatitis B virus in carriers [10], and/or peripheral neuropathy [6].

The tumor microenvironment (TME) of almost all solid tumors is acidic, with the lowest pH reaching 6.0 [11–13]. The pH (low) insertion peptide (pHLIP) family targets the TME, and the targeting is unrelated to the distribution of tumor cell surface receptors [13]. Thus, pHLIP can target a broad spectrum of solid tumors, including TNBC [14, 15]. The method of labeling peptides with radioiodine is simple and established. If pHLIP is labeled with radioiodine, the labeled molecules are specifically distributed in the tumor, and the level of distribution in normal tissues is low, which forms a high-contrast image. In addition, the side effects of using radioactive molecules on intratumoral radiation therapy are milder than those of conventional chemotherapy. Thus, the radioiodine-labeled pHLIP is expected to be used in the imaging and treatment of TNBC to solve the inadequacies of existing diagnoses and treatments of TNBC. In previous studies [16], biodistribution and single photon emission computed tomography (SPECT) imaging showed low binding of [125I] I-pHLIP (Var7) to tumors after pHLIP (Var7) was labeled with 125I, which may be caused by the presence of iodine-binding tyrosine and tryptophan in the pHLIP (Var7) insertion region. Iodine labeling in the insertion region may affect the formation of the α-helix secondary structure of peptides in an acidic environment. Therefore, it is necessary to design a novel peptide for radioiodine labeling.

The structure–activity relationship (SAR) of α-helical peptides (the pHLIP family and antimicrobial peptides) shows that at least seven parameters may affect the efficacy and activity of α-helical peptides: amino acid sequence, number of amino acids, degree of α-helix structures, charge, total hydrophobicity, amphiphilicity, and widths of the hydrophobic and hydrophilic surfaces of the helix [17, 18]. In this study, the sequence of pHLIP (Var7) was modified by a sequence modification method [17] without changing the charge, amino acid number, α-helix, hydrophobicity, and amphiphilicity of the peptide: The

tryptophan of the insertion region was replaced by the nonpolar amino acid phenylalanine, the tyrosine of the insertion region was replaced by the nonionized polar amino acid cysteine, and tyrosine was introduced into the N-terminus of the peptide for radioiodine labeling. Finally, a new sequence, pH (low) insertion peptide variant 7-like peptide (pHLIP (Var7) LP), was obtained: AYEEQNPFARCLEFLFPTETLLLEL.

In this study, 125I was used to label the peptide pHLIP (Var7) LP to verify the feasibility of radioiodine labeling and the targeting of the probe to the TME. Because this study does not involve treatment evaluations, 125I was selected for use because of its lower energy.

Materials and Methods

Materials

Main Instruments

The main instruments used in this study included a Shimadzu-LC2010 high-performance liquid chromatography (HPLC) instrument (Shimadzu Corporation, Japan), an Agilent 6125B mass spectrometer (Agilent Technologies, Inc., USA), a Chirascan plus ACD spectropolarimeter (Applied Photophysics, UK), an Olympus BX51 fluorescence microscope (Olympus Corporation, Japan), a GC-2016 gamma counter (Zhongke Zhongjia Scientific Instrument Co., Ltd., China), a CRC-55tR radiopharmaceutical dose calibrator (Capintec Inc., USA), and a U-SPECT+/CT small-animal SPECT/CT imaging system (MILabs, Netherlands).

Main Reagents

The main reagents used in this study included [125I] NaI (McMaster University, Canada), pierce iodination tubes (Thermo Fisher Scientific, China), isoflurane (Shenzhen RWD Life Technology Co., Ltd., China), a Gemini-NX HPLC column (Phenomenex, USA), and a C18 column (Waters, China).

Cell Culture and Xenograft Model

The human breast cancer cell line MDA-MB-231 (Chinese Academy of Sciences) was cultured in DMEM high glucose medium containing 10% fetal bovine serum and a 1% penicillin and streptomycin mixture at 37 ℃ with 5% CO_2.

Animal studies were approved by the ethics committee of the Affiliated Hospital of Qingdao University, and the management of animals corresponded to animal ethical standards. Female BALB/c nude mice (4–5 weeks old, JOINN Laboratories) were used to establish a tumor model of MDA-MB-231, and 0.1-ml cell suspension containing 1×10^6 MDA-MB-231 cells (50 µl of phosphate-buffered saline (PBS) + 50 µl of Matrigel) was injected into the right armpit of each mouse.

Methods

Characterization of pHLIP (Var7) LP and pHLIP (Var7)

ProtParam was used to analyze the basic parameters of the new peptide, including the amino acid number, charge number, and average hydrophobicity. DNASTAR was used to analyze and predict the secondary structure of the new peptide.

Peptide Synthesis

pHLIP (Var7) LP, pHLIP (Var7) and control peptide kVar7 [19] were synthesized by solid-phase peptide synthesis (SPPS) with molecular weights of 2987.42, 3065.49, and 3062.67, respectively (Shanghai Apeptide Co., Ltd., China). The sequences of the peptides studied were as follows:

pHLIP (Var7) LP: AYEEQNPFARCLEFLFPTETLLLEL;
pHLIP (Var7): ACEEQNPWARYLEWLFPTETLLLEL; and
kVar7: ACEEQNPWARYLKWLFPTKTLLLKL.

Peptides were purified by a Shimadzu-LC2010 HPLC instrument equipped with a Gemini-NX C18 chromatographic column (5 μm, 4.6 × 250 mm) eluted with a gradient from 18 to 100% solvent A (0.1% trifluoroacetic in 100% acetonitrile) and 82 to 0% solvent B (0.1% trifluoroacetic in 100% water) at 1.0 ml/min, with monitoring at 220 nm. The identities of the peptides were confirmed by mass spectrometric analysis using an Agilent 6125B mass spectrometer.

Circular Dichroism (CD) Spectroscopy

The sample preparation was as follows: 7 μmol/l pHLIP (Var7) LP and 2 mmol/l POPC (1-palmitoyl-2-oleoyl-*sn*-glycero-3-phosphocholine; diameter ≤ 50 nm) were combined in 10 mmol/l phosphate buffer (PB) at pH = 8 and then equilibrated at room temperature for at least 10 h. The solution pH was adjusted to 4.0 with 0.1 mol/l HCl. CD spectra of pHLIP (Var7) LP were recorded at pH = 8 and 4 in a 1-mm path-length quartz cuvette using a Chirascan CD spectrometer. The experimental conditions were as follows: bandwidth, 1 nm; wavelength range, 190–400 nm; wavelength step size, 1 nm; time-per-point, 0.5 s; and temperature, 25 °C.

Analysis of Peptide Binding to MDA-MB-231 Cells

5-carboxytetramethylrhodamine (5-TAMRA) (Beijing Bio-Dee Biotechnology Co., Ltd., China) was conjugated to the N-terminus of peptides through solid-phase synthesis. The carboxyl group of 5-TAMAR can undergo condensation reaction with the amino group of the N-terminal amino acid of a peptide. DMEM was mixed with HCl (1 mol/l) to simulate the extracellular culture environment with gradient pH values (pH 7.4, 6.6, and 6.0). A total of 5.0×10^4 MDA-MB-231 cells were seeded in each well of a 24-well plate, and then 0.4 ml of gradient pH cell culture medium containing 50 μg/ml 5-TAMRA-pHLIP (Var7) LP was added to each well. After incubation for 30 min, the cell culture medium was removed, and the wells were washed with PBS (25 mmol/l) at the same pH value 5 times to remove any unbound probes. Then, fluorescence microscopy was used to observe and analyze the fluorescence intensity. The processing steps of 5-TAMRA-pHLIP (Var7) and 5-TAMRA-kVar7 were the same as described above.

Preparation and In Vitro Stability of [125I] I-pHLIP (Var7) LP

pHLIP (Var7) LP was labeled with 125I by the iodogen iodination method. First, 1 mg of pHLIP (Var7) LP powder was dissolved in 1 ml of PB, and 200 μl of the solution was removed for the experiment. Then, 3 μl of [125I] NaI (49.6 MBq) was added, and the solution was mixed well. This solution was then added to the iodogen tube and reacted for 10 min at room temperature on a shaking table. Next, the solution was removed and stabilized in an Eppendorf tube for 5 min and then passed through the activated C18 column. The column was washed with distilled water and then with ethanol, and finally the eluated solution was diluted with PB buffer to obtain [125I] I-pHLIP (Var7) LP.

The radiochemical purity of [125I] I-pHLIP (Var7) LP was determined by paper chromatography [15, 20, 21]. Fifty microliters of purified [125I] I-pHLIP (Var7) LP solution was mixed well with 100 μl of mouse serum and placed in a water bath at 37 °C. The radiochemical purity was measured at 1, 2, and 6 h after mixing.

Biodistribution

When the tumor diameter reached 0.8–1.0 cm, an in vivo distribution experiment was carried out. The tumor-bearing nude mice began to drink 0.1% KI solution 3 days before the experiment to block the thyroid gland until the end of the experiment. Nine tumor-bearing nude mice with no significant difference in tumor size were selected. Each nude mouse was injected with 1.48 MBq/200 μl of [125I] I-pHLIP (Var7) LP via the tail vein. Mice were humanely sacrificed at 1, 2, and 6 h after injection. Major organs/tissues/fluids including the tumor, heart, liver, spleen, lung, kidney, stomach, intestine, muscle, and blood were collected, weighed, and counted using a γ counter. The result is presented as the percentage of injected dose per gram of tissue (% ID/g).

Small-Animal SPECT/CT Scanning

When the tumor diameter reached 0.8–1.0 cm, it was used for imaging. The tumor-bearing nude mice began to drink 0.1% KI solution 3 days before imaging to block the thyroid until the end of the experiment. The tumor-bearing mice were anesthetized with 2% isoflurane before examination ($n = 3$). Then, 3.7 MBq/200 μl of [^{125}I] I-pHLIP (Var7) LP was injected by tail vein, and small-animal SPECT/CT scanning was performed at 1, 2, and 6 h. The small-animal SPECT/CT settings were as follows: time per frame, 10 min; voxel size, 0.8 mm; number of subsets, 32; and number of iterations, 15.

Statistical Analysis

SPSS 24.0.0.0 (IBM) statistical software was used to process the data. The measurement data are expressed as the mean (M) ± standard deviation (SD). One-way analysis of variance (ANOVA) was used for comparisons of variables. $P < 0.05$ was considered statistically significant.

Results

Characterization of pHLIP (Var7) LP and pHLIP (Var7)

ProtParam analysis showed that the amino acid number and charge number of pHLIP (Var7) LP and pHLIP (Var7) were the same, while the grand average of hydropathicity (GRAVY) value of pHLIP (Var7) LP was slightly higher than that of pHLIP (Var7) (Table 1).

DNASTAR analysis showed that both pHLIP (Var7) LP (Fig. 1A) and pHLIP (Var7) (Fig. 1C) had α-helix structures and amphiphilicity. Helical wheel projections show the exact spatial position of polar and nonpolar amino acids in the insertion regions of pHLIP (Var7) LP (Fig. 1B) and pHLIP (Var7) (Fig. 1D) (green represents nonpolar amino acids; red represents polar amino acids), and the maximum hydrophobic angle θ of pHLIP (Var7) LP and pHLIP (Var7) was 80°.

Peptide Synthesis

pHLIP (Var7) LP (Fig. 2A), pHLIP (Var7), and kVar7 were successfully synthesized by the SPPS method and analyzed

Table 1 Basic parameters of pHLIP (Var7) LP and pHLIP (Var7)

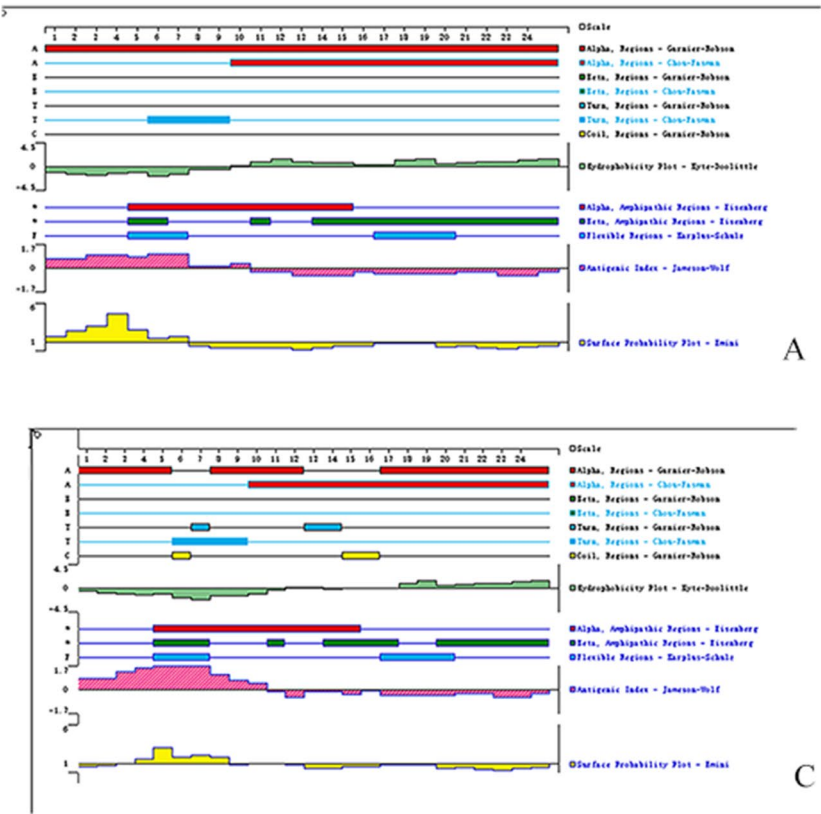| Peptide	Amino acid number	Charge values	Gravy
pHLIP (Var7)	25	− 4	− 0.200
pHLIP (Var7) LP	25	− 4	0.096

Fig. 1 Secondary structure and helical wheel projections of pHLIP (Var7) LP and pHLIP (Var7)

by HPLC and MS. HPLC analysis of pHLIP (Var7) LP indicated the formation of several compounds consisting of a major product (95.1%, retention time of 13.8 min) accompanied by 5 smaller peaks at retention times of 12.9, 13.4, 13.5, 14.4, and 18.0 min (Fig. 2B). The MS analysis of pHLIP (Var7) LP showed 2 mass peaks with m/z values of 867.9 ([M + K + 3H]4+) and 1144.0 ([M + 3H]3+) (Fig. 2C).

CD Spectroscopy

The secondary structure of the peptide was determined by CD at different pH values. Figure 3 shows a typical pH-dependent transition of pHLIP (Var7) LP from an unstructured conformation to an α-helix conformation when the pH decreases from 8.0 (blue line) to 4.0 (red line).

Analysis of Peptide Binding to MDA-MB-231 Cells

5-TAMRA-pHLIP (Var7) LP and 5-TAMRA-pHLIP (Var7) had high binding with MDA-MB-231 cells at pH = 6.0 and 6.6 but only slight binding at pH = 7.4; 5-TAMRA-kVar7 had only slight binding with MDA-MB-231 cells at pH = 6.0, 6.6, and 7.4 (Fig. 4). Semi-quantitative analysis further showed that the relative fluorescence intensities of 5-TAMRA-pHLIP (Var7) LP at pH = 6.0, 6.6, and 7.4 were $100.00 \pm 5.98\%$, $72.10 \pm 4.65\%$ and $13.72 \pm 1.41\%$, respectively; the relative fluorescence intensity in acidic environments was significantly higher than that at pH = 7.4 ($P < 0.01$). The relative fluorescence intensities of 5-TAMRA-pHLIP (Var7) at pH = 6.0, 6.6, and 7.4
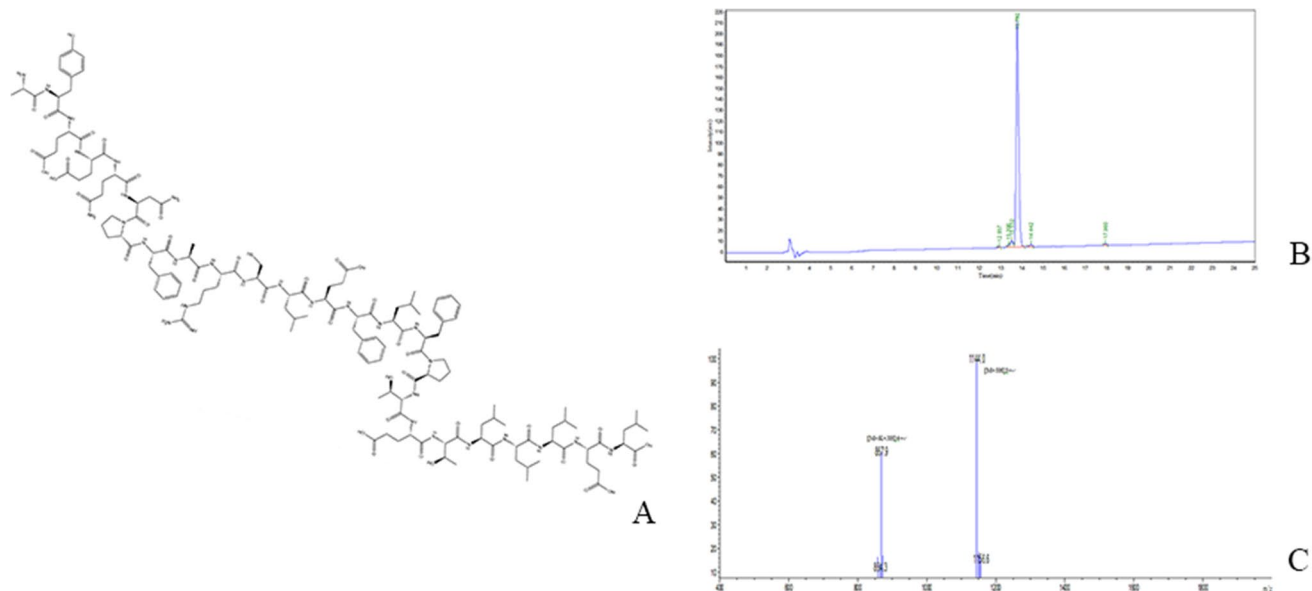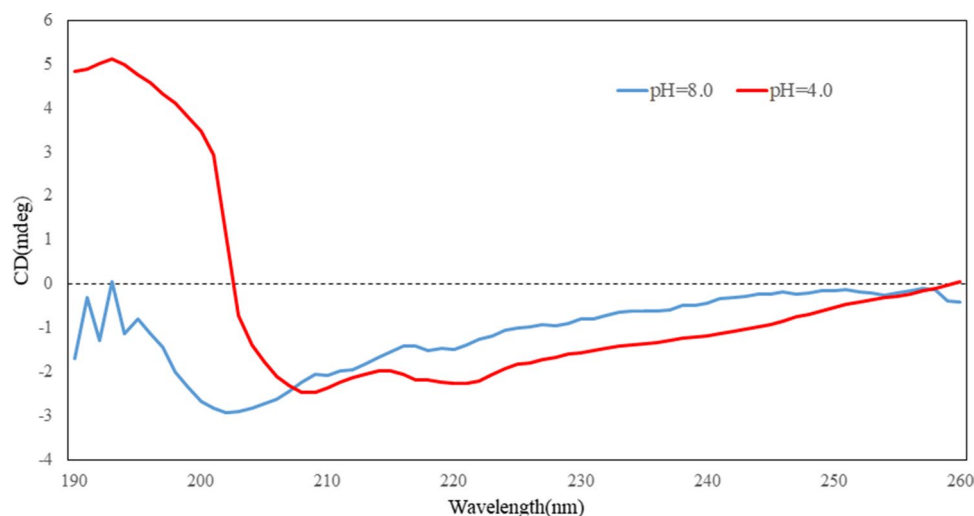

Fig. 2 Molecular structure (**A**), HPLC (**B**), and MS (**C**) analysis of pHLIP (Var7) LP

Fig. 3 CD spectra of pHLIP (Var7) LP. CD spectra were measured in the presence of POPC at pH = 8.0 (blue line) and at pH = 4.0 (red line)
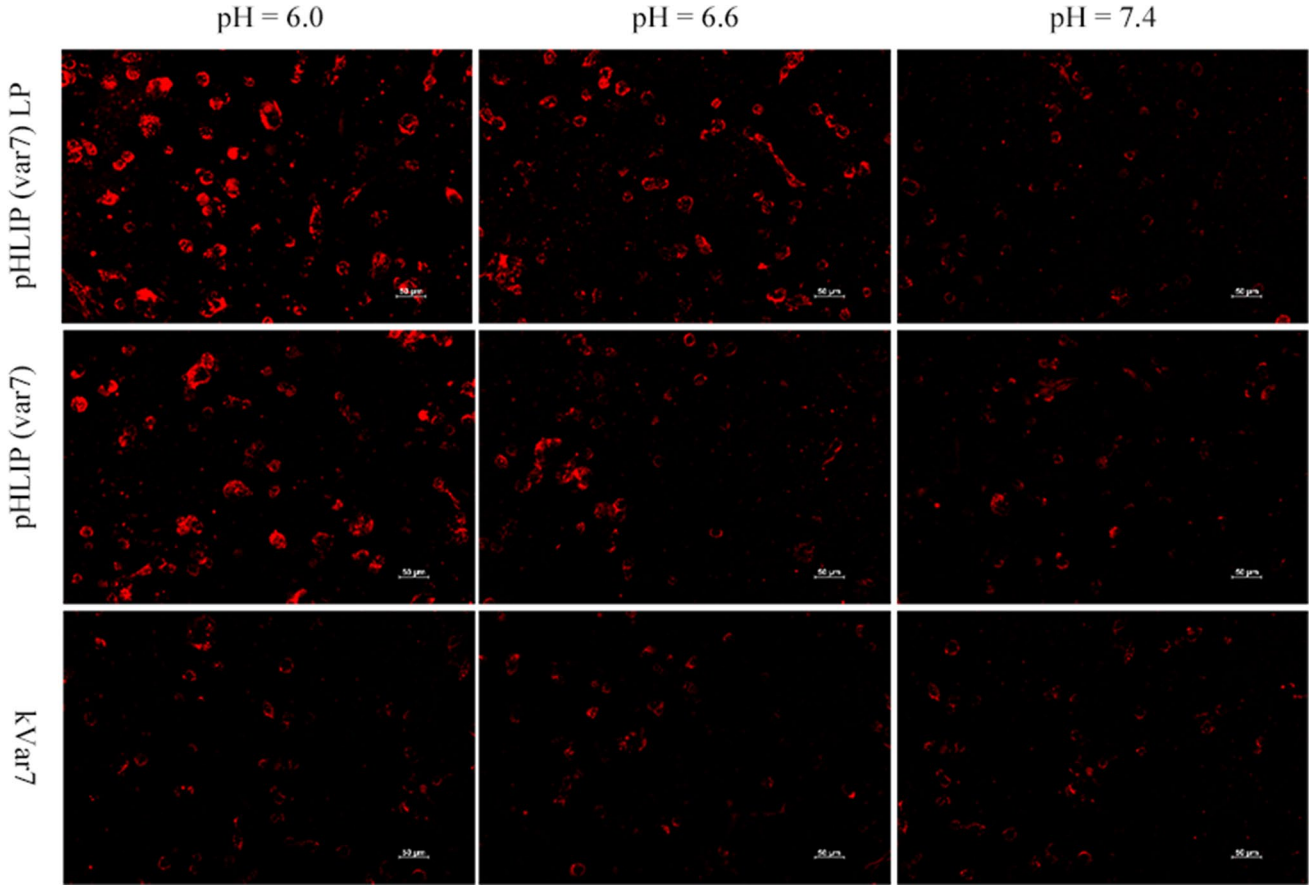
Fig. 4 Fluorescence imaging of pHLIP (Var7) LP, pHLIP (Var7), and kVar7 binding to MDA-MB-231 cells (200×)

were $82.06 \pm 6.43\%$, $47.06 \pm 2.94\%$ and $14.39 \pm 4.09\%$, respectively; the relative fluorescence intensity in the acidic environment was also significantly higher than that at pH = 7.4 ($P < 0.01$). The relative fluorescence intensities of 5-TAMRA-kVar7 at pH = 6.0, 6.6, and 7.4 were $14.78 \pm 1.21\%$, $11.89 \pm 2.19\%$ and $10.62 \pm 2.65\%$, respectively, and there was no significant difference in relative fluorescence intensity at different pH values ($P > 0.05$).

At pH = 6.0 and 6.6, the relative fluorescence intensity values of 5-TAMRA-pHLIP (Var7) LP, 5-TAMRA-pHLIP (Var7), and 5-TAMRA-kVar7 were significantly different ($P < 0.01$); LSD post hoc tests showed that the relative fluorescence intensity of 5-TAMRA-pHLIP (Var7) LP was higher than that of 5-TAMRA-pHLIP (Var7) ($P < 0.01$), and the relative fluorescence intensity values of both 5-TAMRA-pHLIP (Var7) LP and 5-TAMRA-pHLIP (Var7) were higher than that of 5-TAMRA-kvar7 ($P < 0.01$). At pH = 7.4, there was no significant difference in relative fluorescence intensity among 5-TAMRA-pHLIP (Var7) LP, 5-TAMRA-pHLIP (Var7), and 5-TAMRA-kVar7 ($P > 0.05$).

## Preparation and In Vitro Stability of [^{125}I] I-pHLIP (Var7) LP

The radiochemical yield was $40.1 \pm 2.5\%$, and the radiochemical purity was $95.7 \pm 0.1\%$. The molar activity of [^{125}I] I-pHLIP (Var7) LP was 409 ± 22 MBq/μmol.

The radiochemical purity of [^{125}I] I-pHLIP (Var7) LP in mouse serum at 37 ℃ for 1, 2, and 6 h was $94.81 \pm 1.3\%$, $92.73 \pm 2.1\%$, and $87.59 \pm 2.5\%$, respectively.

Biodistribution

Figure 5 summarizes the distribution of [^{125}I] I-pHLIP (Var7) LP in tumor-bearing mice at different time points (A), tumor-to-muscle ratios, and tumor-to-blood ratios (B). Figure 5A shows that the distribution of [^{125}I] I-pHLIP (Var7) LP in tumors reached the highest level at 2 h ($8.7 \pm 1.6\%$ ID/g), and tumor-to-muscle ratios and tumor-to-blood ratios increased with time. The distribution of [^{125}I] I-pHLIP (Var7) LP in off-target organs decreased with time and was relatively higher in the stomach, kidney, and bladder.

Fig. 5 Distribution of [^{125}I] I-pHLIP (Var7) LP in tumor-bearing mice ($n=3$) (**A**) and tumor-to-background ratios (**B**)
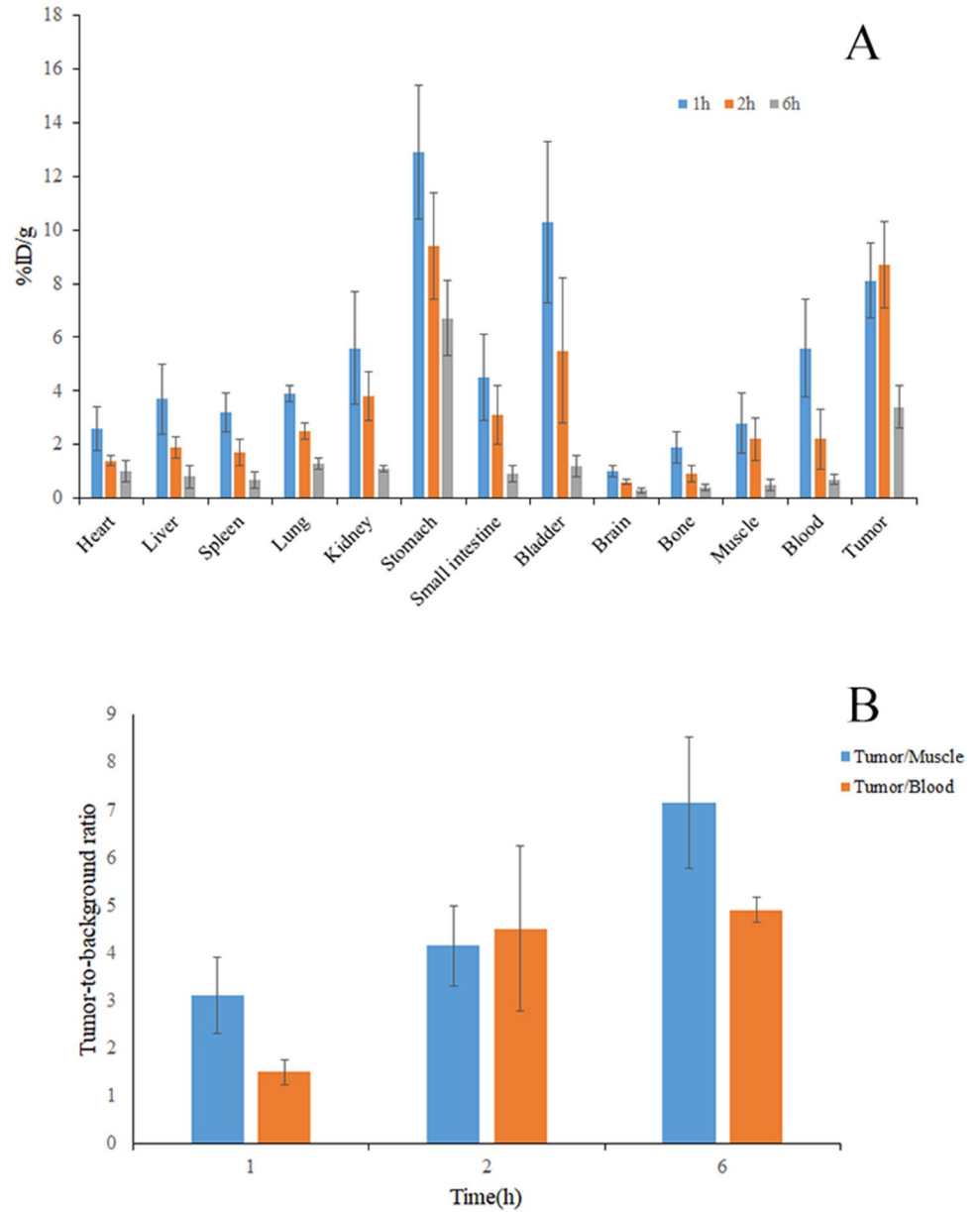
Small-Animal SPECT/CT Scanning

Small-animal SPECT/CT of MDA-MB-231 breast cancer-bearing mice showed that the tumor was imaged clearly at 1 and 2 h after injection of [^{125}I] I-pHLIP (Var7) LP, and the tumor was imaged slightly at 6 h. At 1, 2, and 6 h, the stomach was obviously imaged; the urinary system was obviously imaged at 1 and 2 h (Fig. 6).

Discussion

pHLIP (Var7) LP is obtained by replacing two tryptophans and one tyrosine with two phenylalanines and one cysteine, respectively, in the insertion region of pHLIP (Var7) by the sequence modification method [17]; this method does not change the charge, number of amino acids, α-helix content, hydrophobicity, and amphiphilicity of the peptide. Helical wheel projections show that the positions of polar and non-polar amino acids in the insertion region of pHLIP (Var7) LP and pHLIP (Var7) are the same, suggesting that the insertion regions of pHLIP (Var7) LP and pHLIP (Var7) have the same widths of the hydrophobic and hydrophilic surfaces of the helix. The basic parameters of pHLIP (Var7) LP were analyzed by ProtParam, and it was found that the GRAVY value of pHLIP (Var7) LP was slightly higher than that of pHLIP (Var7), indicating that pHLIP (Var7) LP was slightly more hydrophobic.

CD analysis of pHLIP (Var7) LP indicated the typical pH-dependent transition of pHLIP (Var7) LP from an

Fig. 6 Small-animal SPECT/
CT imaging of [^{125}I] I-pHLIP
(Var7) LP in mice ($n = 3$)
bearing MDA-MB-231 tumors
(arrows)
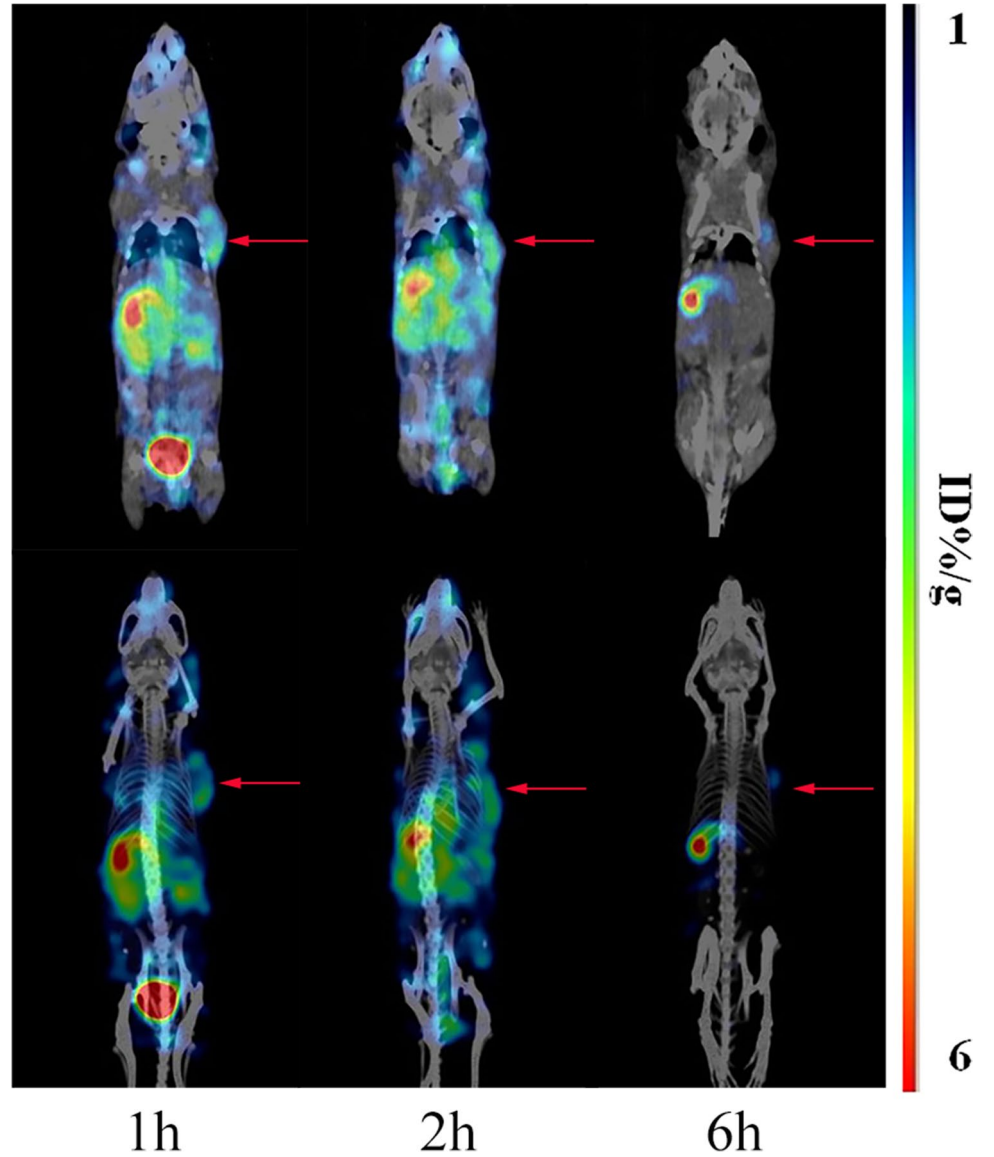
unstructured conformation to an α-helix structure in an acidic environment, which confirmed that the obtained new peptide pHLIP (Var7) LP still had the basic characteristics of the pHLIP family.

The results of binding experiments with MDA-MB-231 cells showed that both pHLIP (Var7) LP and pHLIP (Var7) had high binding levels with MDA-MB-231 cells in acidic environments. Semiquantitative analysis showed that the binding ability of pHLIP (Var7) LP to MDA-MB-231 cells was higher than that of pHLIP (Var7) at pH = 6.0 and 6.6, which may be related to the higher hydrophobicity of pHLIP (Var7) LP than that of pHLIP (Var7); high hydrophobicity is more favorable for peptide insertion into cell membrane. The kVar7 peptide is pH insensitive. Compared with pHLIP (Var7), protonated glutamic acid residues in the insertion region are replaced by positively charged lysine residues and

will not target acidic tissue [19]. This finding is confirmed through binding experiments with MDA-MB-231 cells, to which the kVar7 peptide can only slightly bind at any pH. In this experiment, pH-insensitive 5-TAMRA dye was used to avoid the influence of pH changes on the quantum yield of fluorescence.

pHLIP (Var7) LP can be ^{125}I-labeled by the iodogen iodination method, and the radiochemical purity of [^{125}I] I-pHLIP (Var7) LP in mouse serum at 37 °C for 6 h was still higher than 87%, which met the experimental requirements.

The distribution level of [^{125}I] I-pHLIP (Var7) LP was higher in tumors, and the T/NT ratios increased gradually from 1 to 6 h. On the one hand, this distribution benefits from the fact that the transmembrane action of the pHLIP family is a nonenergy-consuming passive pathway, which is more reliable than the energy-consuming pathway depending on

the active endocytosis of cells. On the other hand, the [125I] I-pHLIP (Var7) LP that did not bind to the tumor in the circulating background was rapidly cleared.

In addition to that in tumors, the distributions of radioactivity in the stomach and urinary system were high. Josefsson et al. [22] showed high expression of sodium/iodide symporter in gastric mucosa, so free iodine would be enriched in the stomach. The high radioactive count in the stomach in this study might be due to the increase in free iodine caused by deiodination of [125I] I-pHLIP (Var7) LP. The high-level distribution of [125I] I-pHLIP (Var7) LP in the urinary system suggested that the urinary system was the main metabolic pathway, which was consistent with the pHLIP family. The pHLIP family is mainly excreted through the urinary system for the following reasons: (1) the kidney is the main metabolic pathway of low molecular weight protein; and (2) normal urine is weakly acidic. The aggregation of the pHLIP family in the kidneys of mice could be reduced by adding weakly alkaline bicarbonate buffer to drinking water [23]. The urinary system, as the main metabolic pathway, is conducive to the removal of probes not combined with tumors, thus improving the image quality of SPECT.

The SPECT imaging and biodistribution results were roughly consistent. The tumor was clearly visible within 2 h postinjection, suggesting that [125I] I-pHLIP (Var7) LP is promising as a TNBC imaging agent. Compared with [125I] I-pHLIP (Var7) [16], the distribution of [125I] I-pHLIP (Var7) LP in the tumor at 1, 2 h was increased (8.1 ± 1.4, $8.7 \pm 1.6\%$ ID/g vs. 6.9 ± 0.4, $3.6 \pm 0.7\%$ ID/g), and the SPECT imaging of the tumor was enhanced, suggesting that changing the position of the radioiodine-labeling of peptides may change tumor targeting. Compared with other studies of pHLIP labeled with radionuclides (^{99m}Tc, ^{64}Cu, ^{18}F) [18, 24, 25], the image background of this study was low, which may be related to the excretion pathway of the tracers: the tracers were mainly excreted through the kidneys, and the remaining tracers were mainly excreted through the hepatobiliary system. The limitation of this study was that the accumulation of tracers in the tumor began to decrease 6 h after the injection, which may be related to the deiodination of [125I] I-pHLIP (Var7) LP. The accumulation of the agent in the stomach was more intense than that in the tumor at every time point, which provided further proof of the deiodination of [125I] I-pHLIP (Var7) LP. Demoin et al. [18] labeled ^{18}F on the side chain of the N-terminal cysteine of pHLIP (Var7), which changed the elimination characteristics of the probe and improved the tumor targeting and image quality of the peptide, which is a noteworthy strategy.

The biodistribution (tumor-to-blood ratios at 1, 2 h, and 6 h were 1.5 ± 0.3, 4.5 ± 1.7, and 4.9 ± 0.3), and SPECT imaging results suggested that [125I] I-pHLIP (Var7) LP was a probe with excellent tumor targeting. However, deiodination is one deficiency of both this probe and other radioiodinated compounds, which limits the application of radioiodinated compounds in tumor imaging and treatment. In future studies, we will adjust the molecular structure of pHLIP (Var7) LP;

for example, we will label radioiodine at the C-terminus of the peptide to transport radioiodine into tumor cells to minimize the impact of deiodination or we will try to connect a tyrosine-containing linker group to the side chain of cysteine of the N-terminus of the peptide to obtain more stable radioiodine-labeled peptide, which may play an active role in promoting the application of radioiodinated compounds in tumor imaging and treatment.

Conclusions

pHLIP (Var7) LP, the new peptide acquired by the sequence modification method, had the typical pH-dependent transition from an unstructured conformation to an α-helix structure and high binding levels with MDA-MB-231 cells in acidic environments. [125I] I-pHLIP (Var7) LP had rapid and sustained tumor uptake in MDA-MB-231 TNBC models. This study provides a new peptide that is more suitable for radioiodine labeling, and we anticipate that our research explores a more effective and promising method for the diagnosis, staging, and treatment of TNBC.

Declarations

Conflict of Interest The authors declare that they have no conflict of interest.

References

1. Pareja F, Reis-Filho JS (2018) Triple-negative breast cancers—a panoply of cancer types. Nat Rev Clin Oncol 15(6):347–348
2. Penault-Llorca F, Viale G (2012) Pathological and molecular diagnosis of triple-negative breast cancer: a clinical perspective. Ann Oncol 23(Suppl 6):vi19-22
3. Aebi S, Davidson T, Gruber G et al (2011) Primary breast cancer: ESMO clinical practice guidelines for diagnosis, treatment and follow-up. Ann Oncol 22(Suppl 6):vi12-24
4. Foulkes WD, Smith IE, Reis-Filho JS (2010) Triple-negative breast cancer. N Engl J Med 363(20):1938–1948
5. Jitariu AA, Cîmpean AM, Ribatti D et al (2017) Triple negative breast cancer: the kiss of death. Oncotarget 8(28):46652–46662
6. Ditsch N, Kolberg-Liedtke C, Friedrich M et al (2021) AGO Recommendations for the Diagnosis and Treatment of Patients with Early Breast Cancer: Update 2021. Breast Care (Basel) 16(3):214–227
7. Bakker MF, de Lange SV, Pijnappel RM et al (2019) Supplemental MRI screening for women with extremely dense breast tissue. N Engl J Med 381(22):2091–2102
8. Elghazaly H, Rugo HS, Azim HA et al (2021) Breast-Gynaecological & Immuno-Oncology International Cancer Conference (BGICC)

Consensus and Recommendations for the Management of Triple-Negative Breast Cancer. Cancers (Basel) 13(9):2262

9. Beusterien K, Grinspan J, Kuchuk I et al (2014) Use of conjoint analysis to assess breast cancer patient preferences for chemotherapy side effects. Oncologist 19(2):127–134

10. Liu Z, Jiang L, Liang G et al (2017) Hepatitis B virus reactivation in breast cancer patients undergoing chemotherapy: a review and meta-analysis of prophylaxis management. J Viral Hepat 24(7):561–572

11. Cairns R, Papandreou I, Denko N (2006) Overcoming physiologic barriers to cancer treatment by molecularly targeting the tumor microenvironment. Mol Cancer Res 4(2):61–70

12. Pathak AP, Gimi B, Glunde K et al (2004) Molecular and functional imaging of cancer: advances in MRI and MRS. Methods Enzymol 386:3–60

13. Penet MF, Glunde K, Jacobs MA et al (2008) Molecular and functional MRI of the tumor microenvironment. J Nucl Med 49(5):687–690

14. Yu M, Chen Y, Wang Z et al (2020) pHLIP (Var7)-P1AP suppresses tumor cell proliferation in MDA-MB-231 triple-negative breast cancer by targeting protease activated receptor 1. Breast Cancer Res Treat 180(2):379–384

15. Chen YH, Yu MM, Wang ZG (2021) Inhibition of MDA-MB-231 cell proliferation by pHLIP (Var7)-P1AP and SPECT imaging of MDA-MB-231 breast cancer-bearing nude mice using 125I-pHLIP (Var7)-P1AP. Nuklearmedizin 60(3):240–248

16. Yu M, Sun Y, Yang G et al (2021) An experimental study on [125I] I-pHLIP (Var7) for SPECT/CT imaging of an MDA-MB-231 triple-negative breast cancer mouse model by targeting the tumor microenvironment. Mol Imaging 2021:5565932

17. Tossi A, Sandri L, Giangaspero A (2000) Amphipathic, alpha-helical antimicrobial peptides. Biopolymers 55(1):4–30

18. Demoin DW, Wyatt LC, Edwards KJ et al (2016) PET imaging of extracellular pH in tumors with (64) Cu- and (18)F-labeled pHLIP peptides: a structure-activity optimization study. Bioconjug Chem 27(9):2014–2023

19. Sosunov EA, Anyukhovsky EP, Sosunov AA et al (2013) pH (low) insertion peptide (pHLIP) targets ischemic myocardium. Proc Natl Acad Sci U S A 110(1):82–86

20. Yu M, Zhou H, Liu X et al (2010) Study on biodistribution and imaging of radioiodinated arginine-arginine-leucine peptide in nude mice bearing human prostate carcinoma. Ann Nucl Med 24(1):13–19

21. MingMing Yu, Wang RongFu, Yan P et al (2008) Design, synthesis and iodination of an Arg-Arg-Leu peptide for potential use as an imaging agent for human prostate carcinoma. J Label Compd Radiopharm 51(11):374–378

22. Josefsson M, Grunditz T, Ohlsson T et al (2002) Sodium/iodide-symporter: distribution in different mammals and role in entero-thyroid circulation of iodide. Acta Physiol Scand 175(2):129–137

23. Andreev OA, Dupuy AD, Segala M et al (2007) Mechanism and uses of a membrane peptide that targets tumors and other acidic tissues in vivo. Proc Natl Acad Sci U S A 104(19):7893–7898

24. Macholl S, Morrison MS, Iveson P et al (2012) In vivo pH imaging with (99m)Tc-pHLIP. Mol Imaging Biol 14(6):725–734

25. Daumar P, Wanger-Baumann CA, Pillarsetty N et al (2012) Efficient (18)F-labeling of large 37-amino-acid pHLIP peptide analogues and their biological evaluation. Bioconjug Chem 23(8):1557–1566